Hole transport in poly(phenylene vinylene)/methanofullerene bulk-heterojunction solar cells

Melzer, C.; Koop, E.J.; Mihailetchi, V.D.; Blom, P.W.M.

Published in:
Advanced Functional Materials

DOI:
10.1002/adfm.200305156

ADVANCED FUNCTIONAL MATERIALS

Hole Transport in Poly(phenylene vinylene)/Methanofullerene Bulk-Heterojunction Solar Cells

By *Christian Melzer*, *Erik J. Koop*, *Valentin D. Mihailetchi*, and *Paul W. M. Blom**

A fundamental limitation of the photocurrent of solar cells based on a blend of poly(2-methoxy-5-(3′,7′-dimethyloctyloxy)-*p*-phenylene vinylene) (MDMO-PPV) and [6,6]-phenyl C_{61}-butyric acid methyl ester (PCBM) is caused by the mobility of the slowest charge-carrier species, the holes in the MDMO-PPV. In order to allow the experimentally observed photocurrents electrostatically, a hole mobility of at least 10^{-8} $m^2 V^{-1} s^{-1}$ is required, which exceeds the observed hole mobility in pristine MDMO-PPV by more than two orders of magnitude. However, from space-charge-limited conduction, admittance spectroscopy, and transient electroluminescence measurements, we found a hole mobility of 2×10^{-8} $m^2 V^{-1} s^{-1}$ for the MDMO-PPV phase in the blend at room temperature. Consequently, the charge-carrier transport in a MDMO-PPV:PCBM-based solar cell is much more balanced than previously assumed, which is a necessary requirement for the reported high fill factors of above 50 %.

1. Introduction

Recent developments in photovoltaic cells based on heterojunctions between organic materials have led to a significant increase in device efficiencies. Photovoltaic cells of a blend of poly(2-methoxy-5-(3′,7′-dimethyloctyloxy)-*p*-phenylene vinylene) (MDMO-PPV) and [6,6]-phenyl C_{61}-butyric acid methyl ester (PCBM) have thereby proven their capacity for solar-cell applications, exhibiting power-conversion efficiencies of around 3 % at the global AM1.5 (air mass 1.5) spectrum.[1,2] In a donor/acceptor organic photovoltaic cell, light absorption results in the formation of excitons that dissociate at the heterojunction interface by an ultrafast electron transfer from the donor to the acceptor (sub-picosecond range).[3,4] By aide of an internal electric field, the photogenerated free holes and electrons are subsequently transported through the donor and acceptor phases to the anode and cathode, respectively, resulting in an external photocurrent density j_{ph}. Since the photocurrent is not solely governed by the generation rate g of free electron–hole pairs, but also by recombination processes, the charge-transport properties of the semiconductor are detrimental for an efficient photoresponse. The recombination probability of free charges in a photovoltaic cell depends on the mean carrier drift length $w_{h/e} = \mu_{h/e} \tau_{h/e} F$ of the holes (h) and electrons (e).[5] Here, μ is the charge-carrier mobility, τ is the charge-carrier lifetime, and F is the internal electric field. Recombination of the free charge carriers is significant, if the mean carrier drift length of one or both charge-carrier species is smaller than the device thickness d. In other words, recombination is important as long as the transit time of the photogenerated charge carriers is longer than their lifetime. However, if both mean carrier drift lengths exceed the thickness of the film (d), no recombination occurs and the electrodes extract all photogenerated charge carriers. In this saturation regime, both electron and hole lifetimes equal the transit times of the charge carriers. The saturated photocurrent density is given by $J_{ph}^{sat} = qgd$, where q is the electron charge.[5,6]

Since the hole mobility of neat MDMO-PPV has previously been reported to be 5×10^{-11} $m^2 V^{-1} s^{-1}$,[7–9] whereas an electron mobility of 2×10^{-7} $m^2 V^{-1} s^{-1}$ has been reported for PCBM,[10] the charge transport in a heterojunction photovoltaic cell based on these materials is expected to be strongly unbalanced. This has a deep impact on the photoresponse of the respective cell. Due to the unbalanced charge-transport properties, holes accumulate to a greater extent in the device than do electrons. Consequently, the electric field increases close to the anode, thereby assisting the extraction of photogenerated holes, as shown in the inset of Figure 1. Under steady-state conditions, the electric field in a region with thickness d_1 is modified to such an extent that the external hole current equals the external electron current. However, in the region d_1, electrons do not neutralize the accumulated holes, which results in a build-up of space-charges. The electrostatic limit of hole accumulation is reached when the photogenerated current density $j_{ph1} = qgd_1$ is equal to the space-charge-limited current dentsity in region d_1:[5]

$$j_{ph1} = qgd_1 \leq j_{SCLC1} = \frac{9}{8} \varepsilon \mu_h \frac{V_1^2}{d_1^3} \quad (1)$$

where j_{SCLC1} is the space-charge-limited current density (SCLC) across the region of strong hole accumulation, V_1 is the voltage drop over this region, and ε is the dielectric permittivity. Since almost the entire voltage V drops in the region of hole accumulation ($V_1 \approx V$), the maximal electrostatically allowed photocurrent density j_{ph}^{max} is given by:[5]

$$j_{ph} \leq j_{ph}^{max} = (qg)^{0.75} \left(\frac{9}{8} \varepsilon \mu_h\right)^{0.25} \sqrt{V} \quad (2)$$

Note that j_{ph}^{max} scales with the square root of the voltage and depends on the charge-carrier mobility of the slower charge-car-

[*] Prof. P. W. M. Blom, C. Melzer, E. J. Koop, V. D. Mihailetchi
Material Science Centre, University of Groningen
Nijenborgh 4, NL-9747 AG Groningen (The Netherlands)
E-mail: p.w.m.blom@phys.rug.nl

 DOI: 10.1002/adfm.200305156

rier species as well as the generation rate of free electron–hole pairs. In order to be able to predict the electrostatic limit, information on g is still required. The magnitude of g can be estimated from the photocurrent density at the transition to the saturation regime.[11] For a typical photovoltaic cell based on MDMO-PPV and PCBM, 2×10^{27} free hole–electron pairs are generated per second and cubic meter, upon illumination with 800 W m^{-2} from a halogen lamp.

In Figure 1, the maximal electrostatically allowed photocurrent density, calculated by considering the reported hole mobility of pristine MDMO-PPV, is plotted (dashed line) as a function of the effective voltage V_{oc}–V. The open-circuit voltage V_{oc} is the voltage at which the photocurrent density equals zero, implying that the electric field in the device is small. The difference between the applied voltage V and V_{oc} therefore represents the effective voltage across the device. Surprisingly, the experimentally observed photocurrent (○) of a photovoltaic cell exceeds its predicted limit by one order of magnitude. This raises the fundamental question: why doesn't the space-charge limit hold? Considering Equation 2, it appears that the observed photocurrent is only electrostatically allowed when the hole mobility in the blend exceeds 10^{-8} m^2 V^{-1} s^{-1} (solid line), which is more than two orders of magnitude above the hole mobility of the neat polymer.

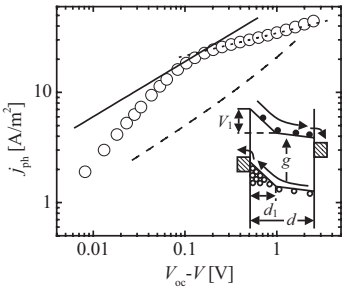

Figure 1. Photocurrent density voltage dependence of an ITO/PEDOT:PSS/MDMO-PPV:PCBM/LiF/Al photovoltaic cell (○). The device thickness was 95 nm. V_{oc} is the open-circuit voltage. The dotted line indicates the saturation current. The dashed line is the space-charge-limited photocurrent calculated by use of the μ_h of neat MDMO-PPV and a generation rate of free electron–hole pairs of 2×10^{27} m^{-3} s^{-1}. The continuous line is the space-charge-limited photocurrent calculated by assuming a μ_h of 10^{-8} m^2 V^{-1} s^{-1}. The inset schematically shows a photovoltaic cell under illumination.

Herein, we report on the determination of the hole mobility in a 1:4 weight-ratio blend of MDMO-PPV and PCBM. We performed current–voltage, transient electroluminescence (EL), and admittance measurements, which unveiled a hole mobility in the MDMO-PPV phase as high as 2×10^{-8} m^2 V^{-1} s^{-1}. This strongly enhanced hole mobility is consistent with the typically observed photoresponse of corresponding photovoltaic cells, since it predicts a conceivable maximal electrostatically allowed photocurrent.

2. Results

2.1. Current–Voltage Measurements

A frequently used tool for investigating charge-carrier mobilities of low mobility media is to examine the space-charge-limited current through a semiconductor in the dark,[7,10] since the SCLC is directly proportional to the charge-carrier mobility:

$$j_{SCLC} = \frac{9}{8} \varepsilon \mu \frac{V^2}{d^3} \quad (3)$$

It has recently been demonstrated that the current density–voltage (J–V) characteristics of an ITO/PEDOT:PSS/MDMO-PPV:PCBM/LiF/Al (ITO: indium tin oxide; PEDOT: poly(3,4-ethylenedioxythiophene); PSS: poly(styrene sulfonate)) photovoltaic cell are comparable to those obtained from electron-only diodes of bare PCBM.[12] This indicates that electrons dominate the transport through a cell and that the effective charge-carrier mobility in a cell equals the electron mobility in PCBM. Consequently, in order to investigate the hole transport through the MDMO-PPV phase in a blend, the electron current through the PCBM phase has to be blocked, for example, by the choice of a high-workfunction cathode such as gold. However, it has been reported that a substantial electron-injection current flows when electrons are injected from gold into PCBM,[12,13] exceeding the typically observed hole current in a device of neat MDMO-PPV. For that reason, it has been assumed that the hole mobility in a blend cannot be determined by examining current densities through devices with a gold electron-blocking contact.[12] From an analysis of injection-limited currents and open-circuit voltages of single-layer PCBM devices, it has been calculated that silver, gold, and palladium form barriers to electron injection of 0.65, 0.76, and 0.94 eV with PCBM, respectively.[13] As a result, palladium is the best alternative for excluding electron injection. In Figure 2, the J–V characteristic of an ITO/PEDOT:PSS/MDMO-PPV:PCBM/Pd device is shown (circles). Note that the applied voltage V is corrected for the built-in voltage V_{bi}. The built-in voltage results from the difference in the workfunction of the anode and the cathode.[13] Surprisingly, the J–V characteristics of the blend not only exceeded the simulated SCLC of a single-layer MDMO-PPV hole-only device (□), but also exceeded the simulated electron injection-limited currents from silver (△) and gold (▽) into PCBM, which are both better electron injectors than palladium. There are two possible explanations for this strongly enhanced current in the blend. First, the observed current was a hole only current, meaning that the hole mobility was strongly enhanced if compared to that of neat MDMO-PPV. Secondly, the observed current was an electron current and the injection-limited electron current from palladium into PCBM was strongly enhanced by the presence of holes, and was therefore not comparable to the injection-limited electron current observed with single-layer PCBM devices.

ADVANCED FUNCTIONAL MATERIALS

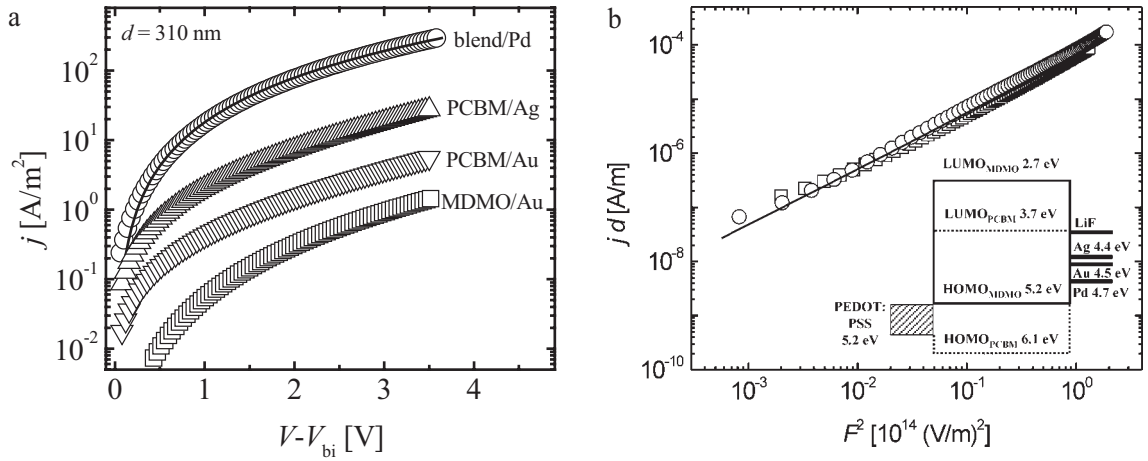

Figure 2. a) *J–V* characteristics of an ITO/PEDOT:PSS/MDMO-PPV:PCBM/Pd device (○). V_{bi} is the built-in potential. The line is a fit using the model of single-carrier SCLC with a field-dependent mobility. Calculated electron-injection currents through ITO/PEDOT:PSS/PCBM/cathode devices with Ag (△) and Au (▽) as the cathode. Parameters were taken from Mihailetchi et al. [13]. Hole-only SCLC through MDMO-PPV (□) were calculated with the parameters previously determined by Blom et al. [7]. b) *J–V* characteristics of an ITO/PEDOT:PSS/MDMO-PPV:PCBM/Pd (□) and an ITO/PEDOT:PSS/MDMO-PPV:PCBM/Ag (○) device. The line is a fit using the model of single-carrier SCLC with a field-dependent mobility. The inset shows the energy diagrams of a cell with various cathode metals [13].

Whether or not the observed current densities in the blend were influenced by electron injection from the cathode into PCBM was verified by changing the cathode metal, thereby altering the charge-injection barriers. In Figure 2, it is shown that the current through a device based on a blend remains unchanged, even when the cathode is changed from palladium to silver. Consequently, any contribution of electrons to the current is highly unlikely, and, in the analysis of the *J–V* characteristics, we regard the device as a hole-only device.

The current densities obtained from an ITO/PEDOT:PSS/MDMO-PPV:PCBM/Pd device scaled quadratically with the applied voltage, which is indicative of space-charge-limited transport (Fig. 2). Assuming that the device is hole-dominated, the *J–V* measurements thus provide information on the hole mobility of the MDMO-PPV phase in the blend. Similar to the findings in neat MDMO-PPV,[7] the hole mobility was field-dependent in a stretched exponential form:

$$\mu_h(F) = \mu_0 \exp\left[\gamma\sqrt{F}\right] \quad (4)$$

where μ_0 is the zero-field hole mobility and γ the field activation factor. μ_0 and γ were determined by simulating the SCLC of the hole-only devices (Fig. 2). At room temperature, a zero-field hole mobility μ_0 of 1.5×10^{-8} $m^2 V^{-1} s^{-1}$ and a field activation factor γ of 1.4×10^{-4} $m^{1/2} V^{-1/2}$ were obtained.

2.2. Admittance Spectroscopy

A powerful technique for investigating charge-transport properties in conjugated polymers is admittance spectroscopy. This technique has already been used for determining transit times (τ_t) and, hence, charge-carrier mobilities of pristine MDMO-PPV.[9] In a diode, where direct current (DC) currents are space-charge-limited, a small alternating current (AC) disturbance of the DC bias changes the space-charge density in the semiconductor, if the frequency ω is below τ_t^{-1}. The space-charge build-up is delayed with respect to the AC stimulus, resulting in an inductive contribution to the capacitance. For frequencies $\omega > \tau_t^{-1}$, the additional space-charge build-up cannot follow the AC stimulus and the geometric capacitance is measured. Consequently, τ_t of the charge carriers is given by the threshold frequency, below which a reduced capacitance is observed. An advantage of this technique is that for devices where both electrons and holes are present, such as in the case of MDMO-PPV-based light-emitting diodes, the respective transport properties can be individually monitored, since they are separated in frequency space.[14]

In Figure 3, it is shown by admittance measurements that ITO/PEDOT:PSS/MDMO-PPV:PCBM/Pd devices exhibit a

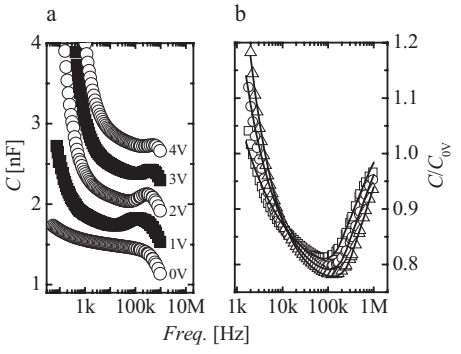

Figure 3. a) Capacitance–frequency plot of an ITO/PEDOT:PSS/MDMO-PPV:PCBM/Pd device at different DC bias. The respective capacitance traces are offset for clarity. The layer thickness was 310 nm. b) Capacitance normalized to zero DC bias capacitance versus frequency for 3 V (□), 3.5 V (○), and 4 V (△) DC bias. The lines are fits with the admittance model for space-charge-limited conduction given by Martens et al. [9].

capacitance decrease below a certain threshold frequency. The fact that an inductive contribution to the capacitance was present confirms that DC currents through these devices were space-charge-limited, since, for a strongly injection-limited device, the amount of injected charge is too small to exhibit an inductive contribution to the capacitance. The observed threshold frequency showed a clear trend upon changes in DC bias. By increasing the DC bias, the threshold frequency was shifted to higher frequencies, reflecting a reduction of the transit time of the charge carriers. From the frequency response of the capacitance, the transit times were determined by simulating the capacitance frequency dependence with a model for space-charge-limited admittance.[9,15] The resulting hole mobilities in the MDMO-phase of the blend for different DC fields are depicted in Figure 5. They are in excellent agreement with the mobilities obtained by simulating the DC SCLC (Fig. 2). Since the mobility of the electrons in the blend is known,[12] the threshold frequency for electron transport can be predicted, and is typically one order of magnitude above the observed threshold frequencies. The absence of any inductive contribution at these higher frequencies is indicative of a hole-dominated device.

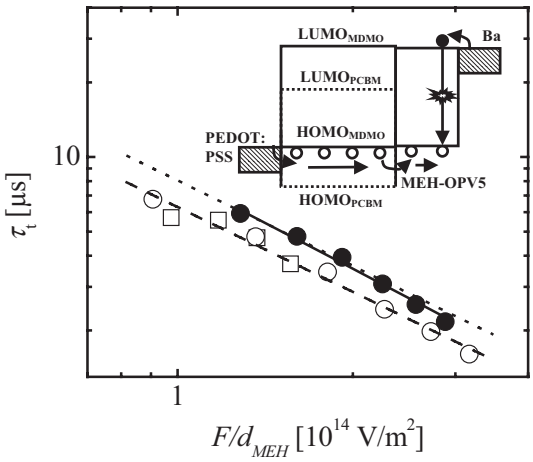

Figure 4. Transit times of holes from EL transient measurements for ITO/PEDOT:PSS/MEH-OPV5/Ba devices with 100 nm (○) and 160 nm (□) layer thickness and an ITO/PEDOT:PSS/MDMO-PPV:PCBM/MEH-OPV5/Ba device with 200 nm layer thickness of the blend and 60 nm layer thickness (d_{MEH}) of MEH-OPV5 (●). The dashed line is a fit using $\tau_t \propto (d/F)^{1/\alpha}$. The dotted line indicates the transit times of double-layer diodes with transport dispersion in the MEH-OPV5 layer, but no dispersion in the blend and a constant hole mobility. The continuous line is a fit using Equations 4–6. The inset schematically shows the operation principle of the EL transient technique in the double-layer configuration.

2.3. Transient Electroluminescence

As a final proof that hole transport in the investigated devices was dominant, and that it is conceivable that the SCLC and admittance spectroscopy unveiled hole mobility in the MDMO-PPV phase, a modified transient electroluminescence (EL) technique was applied. Transient EL has frequently been used to estimate charge-carrier mobilities in highly luminescent organic thin films.[8,16–18] Upon applying a rectangular voltage pulse to a diode, holes and electrons are injected at the corresponding electrodes and traverse the luminescent organic semiconductor until they meet and radiative recombination occurs. A time delay between the onset of the applied voltage and the appearance of the EL is directly related to the transit times of the charge carriers. Advantage can be taken of the fact that hole mobilities in PPV-type materials typically exceed the electron mobilities.[17,19,20] The delay between voltage onset and the appearance of the EL is, therefore, primarily related to the τ_t of the faster charge-carrier species.

As desired in photovoltaic cells, the luminescence in a blend of MDMO-PPV and PCBM is strongly quenched, which complicates the determination of the transit times with EL transient measurements. However, by introducing a luminescent layer between the blend and the cathode, this difficulty can be circumvented. In such double-layer diodes, holes are injected from the anode into the MDMO-PPV phase of the blend and electrons are injected from the cathode into the luminescent layer (Fig. 4). Since radiative recombination exclusively occurs in the luminescent layer, holes have to traverse the entire blend in order to participate in the recombination. Assuming a low electron mobility in the luminescent layer, the time delay between the EL signal and the stimulus (τ_t^{total}) is given by the transit times of holes passing the blend (τ_t^{blend}) and the luminescent layer (τ_t^{lum}):

$$\tau_t^{total} = \tau_t^{blend} + \tau_t^{lum} \quad (5)$$

The PPV-based oligomer (*E*,*E*,*E*,*E*)-1,4-bis[(4-styryl)styryl]-2-methoxy-5-(2′-ethylhexyloxy)benzene (MEH-OPV5) was used as the luminescent layer, since its highest occupied molecular orbital (HOMO) matches that of MDMO-PPV and its electron mobility is known to be below its hole mobility.[18,21] Furthermore, because MEH-OPV5 can be deposited by thermal vacuum deposition, intermixing of the blend and the MEH-OPV5 cover layer is prevented. A high EL brightness at low bias was guaranteed by using PEDOT:PSS as the anode and barium as the cathode.

In order to investigate the transit times of charge carriers passing the blend in a double-layer arrangement, the transit times through the MEH-OPV5 film were first investigated. In Figure 4, the transit times for single-layer MEH-OPV5 devices are shown for film thicknesses of 100 and 160 nm (empty symbols). The revealed transit times are in agreement with those previously reported.[18] The field and thickness dependence of the transit times could be described by $\tau_t \propto (d/F)^{1/\alpha}$ with $\alpha \approx 0.88$, indicating weak dispersivity of the hole transport in MEH-OPV5.[22]

The EL spectrum obtained from a double-layer diode of the blend and MEH-OPV5 was equal to the emission spectrum of a pure MEH-OPV5 layer, confirming that holes did indeed travel through the entire blend. For a double-layer diode with a total thickness of 260 nm, the measured transit times (Fig. 4, solid symbols) were, however, only slightly longer than those

ADVANCED FUNCTIONAL MATERIALS

found for the single-component MEH-OPV5 film. This suggests that the transit times of charge carriers passing the blend were even shorter than those of charge carriers passing the MEH-OPV5 layer. If we convert the observed transit times for the blend directly into a mobility using Equation 6,

$$\mu_h = \frac{d_{blend}}{\tau_t^{blend} F} \quad (6)$$

it appears from Figure 5 (□ and ○) that the obtained hole mobilities are close to those found with both the DC *J–V* measurements and admittance spectroscopy. This indicates that the hole transport through the blend is not (or is only slightly) dispersive. The accordance between mobilities obtained from transient EL measurements and mobilities unveiled by *J–V* and admittance measurements is conclusive proof that the charge transport in ITO/PEDOT:PSS/MDMO-PPV:PCBM/Pd devices is hole-dominated.

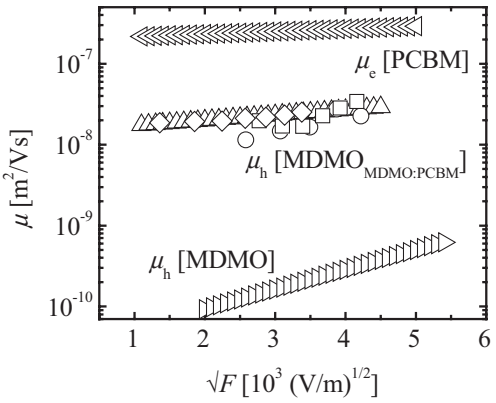

Figure 5. Charge-carrier mobilities versus the square root of the electric field. The hole mobility of neat MDMO-PPV and the electron mobility of neat PCBM were taken from Blom et al. [7] and Mihailetchi et al. [10], respectively. The hole mobilities of the MDMO-PPV phase in the blend with PCBM were obtained by examining the SCLC of hole-only devices (△), by admittance spectroscopy (◇), and by EL transient measurements for 200 nm (□) and 120 nm (○) layer thickness of the blend and 60 nm MEH-OPV5.

3. Discussion

A remarkable agreement between the hole mobilities obtained from DC *J–V* measurements, admittance spectroscopy, and transient EL measurements has been observed (Fig. 5). Accordingly, the room-temperature hole mobility in the blend of MDMO-PPV and PCBM is 2×10^{-8} m^2 V^{-1} s^{-1} for an electric field of 4×10^6 V m^{-1}, which is only one order of magnitude lower than the respective electron mobility in pristine PCBM and 200-fold higher than the hole mobility of the neat polymer. A changed hole mobility in donor-like polymers upon blending with PCBM has already been reported.[23,24] The charge-carrier mobilities in a blend of MDMO-PPV and PCBM were measured, for instance, by Choulis et al., using time-of-flight photocurrent measurements.[24] They reported that the hole mobility in the MDMO-PPV phase of a blend decreases upon adding PCBM below its percolation threshold from 2.4×10^{-10} to 2.3×10^{-11} m^2 V^{-1} s^{-1} at 2.2×10^7 V m^{-1} and increases again above the percolation threshold of PCBM to approximately 2×10^{-10} m^2 V^{-1} s^{-1} for a blend of 1:4 weight ratio of MDMO-PPV/PCBM. Nonetheless, the hole mobility was found to be far below the reported electron mobility in PCBM.[10] Hence, it was believed that space-charge effects restrain the photoresponse of a photovoltaic cell, which is, however, in contradiction to the usually observed photocurrents. Since, for example, a photocurrent governed by a square-root dependence on V (Eq. 2) does not allow fill factors larger than 40 %, the typically observed fill factors of 60 % are inaccessible in a space-charge limit.[1] Yet the hole mobility reported herein is consistent with the reported photoresponse of a cell, exceeding the minimum hole mobility of 10^{-8} m^2 V^{-1} s^{-1}, which is required for an electrostatically allowed photocurrent. Space-charge effects and the concomitant charge-carrier recombination, hence, do not limit the photoresponse, and fill factors of 60 % are conceivable. The discrepancy between the hole mobilities reported here and those of Choulis et al. might be related to differences in the film morphology arising from differences in the sample preparation, which are essential for obtaining the desired devices. Whereas a layer thickness of 1 μm was required for transient photocurrent measurements, the devices we investigated exhibited a layer thickness equal to or smaller than 300 nm, coming closer to the device thickness that is usually used in photovoltaic cells.

Why the hole mobility in the MDMO-PPV increased upon blending the polymer with an excess of PCBM remains an unsolved question. Recently, it has been demonstrated that the charge-carrier mobility in MDMO-PPV as extracted from hole-only diodes and field-effect transistors can differ by more than three orders of magnitude.[25] This large difference originates from the strong dependence of the mobility on the charge-carrier density. However, in the space-charge-limited devices investigated herein, the carrier densities are low and this effect cannot be responsible for the observed mobility increase upon blending with PCBM. Pacios et al. proposed that a change in film morphology upon increased PCBM concentration results in an enhanced intermolecular interaction and, hence, in an improved charge transfer between adjacent molecules.[23] Recent observations on the molecular level concerning the film morphology of MDMO-PPV suggest a similar scenario. It was found that films of MDMO-PPV exhibit interconnected ring-like features, which were attributed to ring-like bent chains, as schematically depicted in Figure 6.[26] The molecular conformation was understood in terms of interactions between adjacent aliphatic side chains on one single chain. Due to the asymmetric side-chain substituents in MDMO-PPV, the interaction causes a bending of the otherwise rigid polymer backbone. Hence, a conformation of the polymer, where substituents of the same species preferably point to one side of the backbone, results in a circular bending of the chain. It has been shown that ring-like, bent polymer chains randomly stack in a pronounced two-dimensional manner. The revealed molecular conformation and the weakly ordered stacking of the molecules might be the origin of the poor transport properties in neat MDMO-PPV, since they are likely to result in a high disorder energy and in poor π–π in-

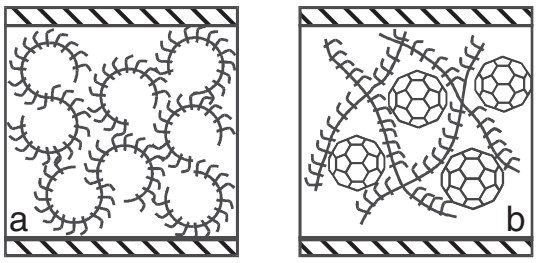

Figure 6. a) The molecular conformation of neat MDMO-PPV according to Kemerink et al. [26]. b) Upon mixing MDMO-PPV with PCBM interactions between the two moieties might change the molecular conformation of MDMO-PPV.

teraction. However, upon blending MDMO-PPV with PCBM, the situation might change, that is, when the formation of the ring-like molecular conformation is hindered due to interactions between MDMO-PPV and PCBM (Fig. 6). On the basis of this assumption, an improvement in the charge-transport properties can be expected, resulting from a reduced nearest-neighbor hopping distance and/or a lower disorder energy. From temperature-dependent measurements, a change in the disorder energy of 0.01 eV could be estimated. Whether this explanation can predict an increase in the hole mobility of more than two orders of magnitude, however, is not clear at present. Modifying the hole-transport properties by systematically changing the chemical structure of the donor-like polymers as well as the PCBM concentration in the blend might give an answer to this question and is the subject of ongoing research. Preliminarily, it can be stated that the hole mobility in symmetric polymers remains unchanged when blended with PCBM. This is expected in the framework of the scenario assumed herein. The results will be discussed in future publications.

4. Conclusion

We have presented consistent experimental evidence that, upon blending MDMO-PPV with PCBM in a 1:4 weight ratio, the hole mobility in the MDMO-PPV phase is enhanced by more than two orders of magnitude, compared to the pristine polymer. Whereas the zero-field hole mobility at room temperature was found to increase strongly, the field activation factor decreased. A hole mobility of around 2×10^{-8} $m^2 V^{-1} s^{-1}$ was disclosed, which is only one order of magnitude lower than the electron mobility in PCBM. Consequently, the charge transport in a bulk-heterojunction solar cell based on MDMO-PPV and PCBM is much more balanced than earlier believed and space-charge build-up is therefore not limiting the photoresponse. Our results shine new light on the high external quantum efficiencies observed in these photovoltaic cells.

Experimental

Device Preparation: Prepatterned ITO-coated glass substrates were wet-cleaned by rubbing with soap, rinsing with water, and ultrasonic cleaning in acetone and propanol. The substrates were further UV-ozone treated and a layer of PEDOT:PSS (Bayer AG) was subsequently spin-coated on the pre-cleaned ITO, using a Convac spin-coater. The PEDOT:PSS layer was dried at an elevated temperature. The samples were then inserted into a glove box filled with nitrogen. A thin layer of a blend of MDMO-PPV:PCBM in a weight ratio of 1:4 was then spin-coated from a chlorobenzene solution with a Karl Suss spin-coater. For transient EL measurements, a thin MEH-OPV5 layer was subsequently vacuum-deposited at 10^{-6} mbar on the blend. Finally, top contacts were deposited via vacuum deposition at 10^{-6} mbar.

Device Characterization: All measurements were performed under a nitrogen atmosphere. *J–V* measurements were performed with a Keithley 2400 Sourcemeter and admittance spectroscopy with an Agilent 4284 A Precision LCR Meter. For transient EL measurements, an HP 8114 A Pulse Generator was used to apply step-like voltage pulses on the samples; the integrated light output was measured with a Keithley 6514 System Electrometer. A detailed description of the transient EL measurements has been given by Blom and Vissenberg [16].

Received: November 28, 2003
Final version: March 25, 2004

[1] S. E. Shaheen, C. J. Brabec, N. S. Sariciftci, F. Padinger, T. Fromherz, J. C. Hummelen, *Appl. Phys. Lett.* **2001**, *78*, 841.
[2] T. Munters, T. Martens, L. Goris, V. Vrindts, J. Manca, *Thin Solid Films* **2002**, *403*, 247.
[3] N. S. Sariciftci, L. Smilowitz, A. J. Heeger, F. Wudl, *Science* **1992**, *258*, 1474.
[4] J. C. Brabec, G. Zera, N. S. Saritiftci, *Chem. Phys. Lett.* **2001**, *340*, 232.
[5] A. M. Goodman, A. Rose, *J. Appl. Phys.* **1971**, *42*, 2823.
[6] R. Sokel, R. C. Hughes, *J. Appl. Phys.* **1982**, *53*, 7414.
[7] P. W. M. Blom, M. J. M. de Jong, M. G. van Munster, *Phys. Rev. B* **1997**, *55*, R656.
[8] M. C. J. M. Vissenberg, P. W. M. Blom, *Synth. Met.* **1999**, *102*, 1053.
[9] H. C. F. Martens, H. B. Brom, P. W. M. Blom, *Phys. Rev. B* **1999**, *60*, R8489.
[10] V. D. Mihailetchi, J. K. J. van Duren, P. W. M. Blom, J. C. Hummelen, R. A. J. Janssen, J. M. Kroon, M. T. Rispens, W. J. H. Verhees, M. M. Wienk, *Adv. Funct. Mater.* **2003**, *13*, 43.
[11] C. L. Braun, *J. Chem. Phys.* **1984**, *80*, 4157.
[12] J. K. J. van Duren, V. D. Mihailetchi, P. W. M. Blom, T. van Woudenbergh, J. C. Hummelen, M. T. Rispens, R. A. J. Janssen, M. M. Wienk, *J. Appl. Phys.* **2003**, *94*, 4477.
[13] V. D. Mihailetchi, P. W. M. Blom, J. C. Hummelen, M. T. Rispens, *J. Appl. Phys.* **2003**, *94*, 6849.
[14] H. C. F. Martens, J. N. Huiberts, P. W. M. Blom, *Appl. Phys. Lett.* **2000**, *77*, 1852.
[15] H. C. F. Martens, *Ph.D. Thesis*, University of Leiden, Leiden **2000**.
[16] P. W. M. Blom, M. C. J. M. Vissenberg, *Phys. Rev. Lett.* **1998**, *80*, 3819.
[17] D. J. Pinner, R. H. Friend, N. Tessler, *J. Appl. Phys.* **1999**, *86*, 5116.
[18] C. Melzer, V. V. Krasnikov, G. Hadziioannou, *J. Polym. Sci., Part B: Polym. Phys.* **2003**, *41*, 2665.
[19] L. Bozano, S. A. Carter, J. C. Scott, G. G. Malliaras, P. J. Brock, *Appl. Phys. Lett.* **1999**, *74*, 1132.
[20] J. C. Scott, P. J. Brock, J. R. Salem, S. Ramos, G. G. Malliaras, S. A. Carter, L. Bozano, *Synth. Met.* **2000**, *111*, 289.
[21] S. C. Veenstra, U. Stalmach, V. V. Krasnikov, G. Hadziioannou, H. T. Jonkman, A. Heeres, G. A. Sawatzky, *Appl. Phys. Lett.* **2000**, *76*, 2253.
[22] H. Scher, E. W. Montroll, *Phys. Rev. B* **1975**, *12*, 2455.
[23] R. Pacios, D. D. C. Bradley, J. Nelson, C. J. Brabec, *Synth. Met.* **2003**, *137*, 1469.
[24] S. A. Choulis, J. Nelson, Y. Kim, D. Poplavskyy, T. Kreouzis, J. R. Durrant, *Appl. Phys. Lett.* **2003**, *83*, 3812.
[25] C. Tanase, E. J. Meijer, P. W. M. Blom, D. M. de Leeuw, *Phys. Rev. Lett.* **2003**, *91*, 216 601.
[26] M. Kemerink, J. K. J. van Duren, P. Jonkheijm, W. F. Pasveer, P. M. Koenraad, R. A. J. Janssen, H. W. M. Salemink, J. H. Wolter, *Nano Lett.* **2003**, *3*, 1191.

